Int. J. Cancer: **120,** 796–805 (2006)

Inflammation and IGF-I activate the Akt pathway in breast cancer

Robyn L. Prueitt[1], Brenda J. Boersma[1], Tiffany M. Howe[1], Julie E. Goodman[2], Douglas D. Thomas[3], Lei Ying[4], Candice M. Pfiester[1], Harris G. Yfantis[5], John R. Cottrell[6], Dong H. Lee[5], Alan T. Remaley[7], Lorne J. Hofseth[4], David A. Wink[3] and Stefan Ambs[1]*

[1]*Laboratory of Human Carcinogenesis, Center for Cancer Research, National Cancer Institute, Bethesda, MD*
[2]*Gradient Corporation, Cambridge, MA*
[3]*Radiation Biology Branch, Center for Cancer Research, National Cancer Institute, Bethesda, MD*
[4]*Laboratory of Inflammatory-Driven Carcinogenesis, Department of Basic Pharmaceutical Sciences, South Carolina College of Pharmacy, Columbia, SC*
[5]*Pathology and Laboratory Medicine, Baltimore Veterans Affairs Medical Center, Baltimore, MD*
[6]*Department of Pathology, University of Maryland School of Medicine, Baltimore, MD*
[7]*Department of Laboratory Medicine, Clinical Center, National Institute of Health, Bethesda, MD*

Akt signaling may promote breast cancer progression and poor disease outcome. We hypothesized that serum insulin-like growth factor I (IGF-I) and a proinflammatory tumor environment induce phosphorylation of Akt and downstream targets of Akt in breast cancer. We studied the relationship between Akt pathway activation, IGF-I and markers of inflammation, *e.g.*, nitric oxide synthase-2 (NOS2), cyclooxygenase-2 (COX2) and tumor phagocyte density, in 248 breast tumors. We also examined the association of Akt phosphorylation with breast cancer survival. We observed that phosphorylation of Akt, BAD and caspase-9 correlated strongly with the expression of the 2 proinflammatory enzymes, NOS2 and COX2, in breast tumors ($p < 0.001$; Spearman rank correlation). Both NOS2 and COX2 expression were independently associated with Akt phosphorylation in the multivariate analysis. Serum IGF-I concentrations and the IGF-I/IGFBP3 ratio correlated with Akt phosphorylation at Thr308 and Ser473 in breast tumors ($p \leq 0.05$; Spearman rank correlation). The association with Akt phosphorylation at Thr308 remained statistically significant in the multivariate analysis. Akt pathway activation was not associated with overall survival in the unstratified analysis, but we observed a statistical interaction between Akt phosphorylation and tumor phagocyte density on breast cancer survival ($p_{interaction} < 0.05$). We further corroborated our findings in cell culture models by demonstrating that ANA-1 macrophages, nitric oxide and prostaglandin E_2 induce Akt phosphorylation in human breast cancer cells. In summary, a proinflammatory environment was found to activate the Akt pathway in breast cancer, and may modify the association between the Akt phosphorylation status and breast cancer survival.

Key words: breast cancer; Akt; inflammation; insulin-like growth factor; survival

The Akt family of serine/threonine protein kinases are putative oncogenes that enhance the survival of various cell types.[1,2] The 3 closely related Akt isoforms induce cell proliferation and soft agar growth, and disrupt the acinar architecture of human mammary cells, but do not induce transformation by themselves.[3–5] Akt activation requires 2 critical phosphorylation steps at Thr308 and Ser473. The phosphorylation is induced by ligand-mediated activation of growth factor receptors and receptor tyrosine kinases. Insulin-like growth factor I (IGF-I), insulin and the epidermal growth factor are ligands that activate Akt through the receptor-mediated pathway.[1,6] The phosphorylation of membrane-bound Akt establishes the full Akt kinase activity and induces Akt translocation into the cytosol and nucleus.[7–10] Activated Akt phosphorylates a number of downstream targets such as BAD, caspase-9, p21, p27, GSK3β, Mdm2, mTOR, IKKα and others.[1,11,12] The phosphorylation of BAD and caspase-9 blocks the apoptotic activity of the 2 proteins and raises the threshold for apoptosis.[13–15] Thus, tumors that show a high phosphorylation of BAD and caspase-9 may have a poor response to treatment.

Several key pathways in breast cancer biology activate the Akt pathway.[4,16–18] Akt expression is upregulated in breast tumors and the phosphorylation of Akt is associated with poor disease-free survival.[19–21] We pursued the hypothesis that a proinflammatory tumor environment increases Akt phosphorylation in breast tumors. It has previously been observed that cyclooxygenase-2 (COX2)-specific inhibitors disrupt Akt signaling in breast cancer cells.[22] We also examined the relationship between serum IGF-I and Akt phosphorylation in breast tumors. Serum IGF-I is a breast cancer risk factor that may enhance tissue inflammation.[23–26] We examined immunohistochemically the phosphorylation of Akt, BAD and caspase-9 in relation to nitric oxide synthase-2 (NOS2) and COX2 expression, tumor phagocyte density, and serum IGF-I. We also assessed the relationship between serum IGF-I and tissue inflammation, and examined possible interactions between these markers and the tumor Akt phosphorylation status in breast cancer survival.

Material and methods

Collection of tumor specimens and survival information

Paraffin-embedded surgical biopsy specimens, blood samples and survival information were obtained from 248 breast cancer cases at the University of Maryland Medical Center, Baltimore Veterans Affairs Medical Center, Union Memorial Hospital, Mercy Medical Center and Sinai Hospital in Baltimore, Maryland. The women were recruited between February of 1993 and August of 2003.[27] Cases were eligible if they resided in the greater Baltimore area at the time of recruitment, were of African-American or Caucasian descent by self-report, had pathologically confirmed breast cancer, were diagnosed with breast cancer within the last 6 months prior to recruitment and had no previous history of breast cancer. Patients were excluded if they were HIV, HCV or HBV carriers, were IV-drug users, were institutionalized, or were physically or mentally unable to sign consent and complete the questionnaire. Of the eligible patients that were identified through surgery lists, 83% participated in the study. The subjects signed a consent form and completed an interviewer-administered questionnaire. The questionnaire evaluated the medical, reproductive, family and occupational history of the subjects. Additional information to determine body mass index (BMI), tumor size, node status, disease stage, treatment and survival was obtained from medi-

Sponsor: Intramural Research Program of the NIH, National Cancer Institute, Center for Cancer Research.
***Correspondence to:** Laboratory of Human Carcinogenesis, National Cancer Institute, Bldg. 37/Room 3050B, Bethesda, MD 20892-4258, USA. E-mail: ambss@mail.nih.gov
Received 1 March 2006; Accepted after revision 21 August 2006
DOI 10.1002/ijc.22336
Published online 9 November 2006 in Wiley InterScience (www.interscience.wiley.com).

cal records and pathology reports, State of Maryland records, the Social Security Death Index and the National Death Index. The Institutional Review Boards at the participating institutions approved the protocol.

Histology evaluation

A pathologist reviewed H&E-stained sections of each tumor specimen, to confirm the presence of tumor and the histology. Disease staging was performed according to the tumor-node-metastasis (TNM) system (AJCC/UICC).

Immunohistochemistry evaluation

Formalin-fixed and paraffin-embedded 5-μm slides were deparaffinized and placed into citrate buffer for antigen retrieval. Slides were microwaved and rinsed in phosphate-buffered saline (PBS) buffer. Endogenous peroxidase was blocked using the DakoCytomation Envision System-HRP blocking buffer, according to the manufacturer's protocol (DakoCytomation, Carpinteria, CA). Protein expression and phosphorylation were evaluated using the following primary antibodies: 1:25 diluted rabbit polyclonal antibody (no. 9277; Cell Signaling Technology, Beverly, MA) for phosphorylated Akt (Ser^{473}); 1:80 diluted monoclonal antibody 244F9 (no. 4056; Cell Signaling Technology) for phosphorylated Akt (Thr^{308}); 1:100 diluted rabbit polyclonal antibody (no. 9295; Cell Signaling Technology) for phosphorylated Bad (Ser^{136}); 1:250 diluted rabbit polyclonal antibody (no. SC-11755; Santa Cruz Biotechnology, Santa Cruz, CA) for phosphorylated caspase-9 (Ser^{196}); 1:50 diluted monoclonal antibody (no. 610204; BD Biosciences/Transduction Laboratories, San Diego, CA) for COX2; 1:250 diluted monoclonal antibody (no. 610328; BD Biosciences/Transduction Laboratories) for NOS2; 1:100 diluted monoclonal DO-7 antibody (DakoCytomation) for p53; 1:100 diluted rabbit polyclonal antibody (DakoCytomation) for c-erbB-2 (HER2/neu); ready-to-use monoclonal Ab-3 antibody (Lab Vision, Fremont, CA) for CD68; and ready-to-use monoclonal (Clone 6F11) antibody (Ventana Medical Systems, Tucson, AZ) for the estrogen receptor (ER). After an overnight incubation with the primary antibody at 4°C, slides were washed in 1× PBS and incubated with a corresponding HRP-labeled secondary antibody, using the DakoCytomation Envision System reagents. Slides were washed after 30-min incubation at room temperature, were stained with DAB and counterstained with Methyl Green. Staining specificity was determined with negative and positive control slides and, if available, with blocking peptides that were purchased from the manufacturer. Phosphospecific peptides were available for phosphorylated Akt (pAkt) at Thr308 and Ser473, and phosphorylated caspase-9 at Ser196. To minimize staining variability, one person performed the immunostaining using a standard protocol. Images of stained sections were taken with the Olympus DP70 Digital Camera System (Olympus, Melville, NY).

Evaluation of the immunohistochemistry data

A combined score of intensity and distribution was used to categorize the immunohistochemical (IHC) staining for protein expression and phosphorylation, with the exception of the p53 and ER IHC. Intensity received a score of 0–3 if the staining was negative, weak, moderate or strong. The distribution received a score of 0–4 if the staining distribution was <10% positive cells, 10–30%, >30–50%, >50–80% and >80%. A sum score was then divided into 4 groups as follows: (*i*) negative = 0–1, (*ii*) weak = 2–3, (*iii*) moderate = 4–5 and (*iv*) strong = 6–7, according to standard protocols for IHC analysis.[28,29] The ER and p53 status were scored negative/positive. p53 expression was scored positive if >10% of the tumor cells expressed nuclear p53. The ER status was determined according to the reference range set by the ChromaVision® ACIS® assisted quantitative image analysis software (Clarient Diagnostic Services, Irvine, CA). The number of phagocytes in the tumor specimens was determined by counting the number of CD68-positive monocytes per 250× field in 3 representative fields.

IGF-I, IGF-II and IGFBP3 serum concentrations

Serum samples were available for 104 cases. IGF-I, IGF-II and IGFBP3 serum concentrations were determined as the average of duplicate measurements, using the Active® IGF-I, IGF-II and IGFBP3 ELISA kits, according to the manufacturer's protocol (Diagnostic Systems Laboratories, Webster, TX). The IGF-I serum concentration was also determined in the Department of Laboratory Medicine, NIH, using the Quest Diagnostics Nichols Institute IGF-I chemiluminescent assay (Nichols Institute Diagnostics, San Clemente, CA). The assays at the 2 laboratories produced highly correlative data ($r^2 = 0.98$, $p < 0.0001$).

Coculture of human breast cancer cells with ANA-1 mouse macrophages

MCF-7 cells were seeded at 2×10^5 cells in 6-well plates and grown in RPMI medium with 4.5 g/l glucose, 2 mM glutamine and 10% FBS. The cells were grown to 80% confluence and serum-starved overnight. ANA-1 cells were cultured in high glucose DMEM + 10% FBS and activated overnight with interferon-γ (10 ng/ml) followed by LPS (10 ng/ml) for 4 hr. ANA-1 cells were harvested and added to the serum-starved MCF-7 cells at a 1:1 ratio. The coculture was stopped at 1, 2 and 4 hr when the cell culture medium was removed, and the MCF-7 cells were washed twice with cold PBS, pH = 7.4, and solubilized with cold lysis buffer (50 mM Tris/HCl, pH = 7.5, 5 mM EDTA, 150 mM NaCl, 1% Triton-X-100 and a protease inhibitor mix). Most of the ANA-1 cells are removed from the coculture during the washing steps with PBS. The coculture experiments with MDA-MB-231 cells were conducted according to a previously published protocol[30] with the following modifications: MDA-MB-231 cells were separated from the ANA-1 cells using the MACS Separator System (Miltenyi Biotec, Auburn, CA). Briefly, following coculture, cells were trypsinized, counted and washed 2× with PBS. Cells were resuspended in 80 μl separation buffer (PBS, 2 mM EDTA, 0.5% BSA) per 1×10^7 cells plus 20 μl anti-mouse CD45 beads. The mixture was incubated at 4°C for 15 min. The MACS Separator column was placed into a miniseparator, and 0.5 ml buffer was added to the column to balance, and to allow for flow through. The cell mixture was washed with 1 ml separation buffer and centrifuged. The pellet was resuspended with 80 μl separation buffer per 1×10^7 cells and added to the column. Cells flowing through were collected, and the column was washed 3 times with separation buffer. The cell suspension was centrifuged, and the supernatant discarded. The pellet of separated, purified MDA-MB-231 cells was stored at −80°C until analysis.

Treatment of human breast cancer cells with SPER/NO, prostaglandin E_2 and okadaic acid

MCF-7 cells and MDA-MB-231 cells were grown to 70% confluency in 100-mm plates in RPMI medium with 2 g/l glucose, 2 mM glutamine and 10% FBS, and DMEM medium with 4.5 g/l glucose, 2 mM glutamine, 1 mM sodium pyruvate and 10% FBS, respectively. Cells were treated with either 25 μM SPER/NO (Alexis Biochemicals, San Diego, CA) or 5 μM prostaglandin E_2, (Sigma-Aldrich, St. Louis, MO). MCF-7 cells were treated with 10 nM okadaic acid and MDA-MB-231 cells with 100 nM okadaic acid (Calbiochem, San Diego, CA). A third cell line, MDA-MB-157, was only treated with 25 μM SPER/NO.

Western blot analysis

Protein concentrations were determined with the Bio-Rad Protein Assay (Bio-Rad Laboratories, Hercules, CA). Western blot analysis was performed according to standard procedures, and 50 μg of total protein was loaded per lane. The protein bands were visualized using the SuperSignal West Pico Chemiluminescent Substrate (Pierce, Rockford, IL). The following antibodies were used to detect

TABLE I – SUMMARY OF TUMOR IHC AND SERUM MARKER ANALYSIS

	n	%
p-Akt (Thr^{308})		
Negative	14	6
Weak	24	10
Moderate	71	29
Strong	134	55
p-Akt (Ser^{473})		
Negative	17	7
Weak	29	12
Moderate	59	24
Strong	142	57
p-BAD (Ser^{136})		
Negative	43	17
Weak	41	17
Moderate	76	31
Strong	85	35
p-Caspase-9 (Ser^{196})		
Negative	38	15
Weak	30	12
Moderate	73	30
Strong	106	43
Cyclooxygenase-2		
Negative	75	30
Weak	83	34
Moderate	65	26
Strong	25	10
Nitric oxide synthase-2		
Negative	43	17
Weak	32	13
Moderate	72	29
Strong	101	41
Nuclear p53		
Negative	173	70
Positive	75	30
CD68-positive phagocytes[1] ($n = 247$)	97 ± 57	
Serum IGF-I[2] (mean ± SD)	176 ± 84	
Serum IGF-II[2] (mean ± SD)	695 ± 219	
Serum IGFBP3[2] (mean ± SD)	4419 ± 1123	
IGF-I/IGFBP3 ratio (mean ± SD)	0.04 ± 0.014	

[1]Per 250× field, mean ± SD.–[2]In nanogram/milliliters; $n = 104$.

TABLE II – DEMOGRAPHIC AND CLINICOPATHOLOGICAL FEATURES OF CASES[1]

	n
Age at diagnosis (mean ± SD; $n = 248$)	55.0 ± 13.9
Body mass index (mean ± SD; $n = 248$)	29.1 ± 8.0
Race	
African-American	143 (58)
Caucasian	105 (42)
Menopausal status[2]	
Premenopausal	64 (31)
Postmenopausal	141 (69)
Smoking[3]	
Ever	118 (52)
Never	111 (48)
Survival	
Alive	189 (76)
Deceased	59 (24)
Tumor histology	
Ductal	189 (76)
Lobular	34 (14)
Others	25 (10)
Stage at diagnosis (TNM)	
≤ Stage I	66 (29)
Stage II	118 (52)
≥ Stage III	44 (19)
Node status	
Negative	144 (63)
Positive	86 (37)
Neoadjuvant therapy	
No	178 (77)
Yes	53 (23)
Chemotherapy	
No	99 (43)
Yes	132 (57)
Estrogen receptor	
Negative	102 (41)
Positive	145 (59)
Her2/neu	
Low to weak	154 (62)
Moderate to strong	93 (38)

[1]Cases with missing information are not included. Values are number (percentage) unless otherwise indicated.–[2]Premenopausal: still having menstruation; postmenopausal: 55 years or older, or stated change of life, or hysterectomy with both ovaries removed.–[3]Ever: smoked more than 6 months in life.

the membrane-bound proteins: rabbit polyclonal anti-pAkt Ser473 from Cell Signaling, 1:500 (no. 9271); rabbit polyclonal anti-pAkt Thr308 from Cell Signaling, 1:250 (no. 9275); rabbit polyclonal anti-Akt from Cell Signaling, 1:2,000 (no. 9272); rabbit polyclonal anti-pGSK3β Ser9 from Cell Signaling, 1:500 (no. 9336); rabbit polyclonal anti-NOS2 from Cayman Chemical, Ann Arbor, MI, 1:400 (no. 160862); monoclonal anti-COX2 from BD Biosciences/Transduction Laboratories, 1:250 (no. 610204).

Statistical analysis

Stata 7.0 (Stata, College Station, TX) and SAS 8.0 (SAS Institute, Cary, NC) statistical softwares were used for data analysis. All statistical tests were 2-sided, and an association was considered statistically significant with $p < 0.05$. The Spearman correlation coefficient was calculated for correlation analyses. The χ^2 test and multivariate logistic regression were performed to analyze dichotomized data and to calculate adjusted odds ratios, respectively. To generate dichotomized data for IHC, scores were divided into moderate to strong *versus* negative to weak, or into strong *versus* negative-moderate. The phosphorylation status of Akt, BAD and caspase-9 was dichotomized into strong *versus* negative to moderate in the logistic and Cox regression analyses, because most tumors had a moderate to strong phosphorylation score for these proteins (Table I). Continuous data, such as serum protein concentrations, BMI or CD68 count, were dichotomized using the median value as the cutoff. Survival analysis was conducted in univariate and multivariate modes. The Kaplan–Meier method and the log-rank test were used for univariate survival analysis. The Cox Proportional-Hazards regression was used for multivariate survival analysis to calculate adjusted hazard ratios. Proportional-hazards assumptions were verified by log–log plots and with the non-zero slope test of the scaled Schoenfeld residuals. A statistical test for interaction was performed to determine whether the effect of Akt phosphorylation on breast cancer survival is modified by other factors. In this test, Akt phosphorylation was coded as zero (negative to moderate IHC) and one (strong IHC). Survival was determined for the time period from the date of hospital admission to the last completed search for death entries in the Social Security Death Index (August 18, 2004). The mean follow-up time for breast cancer survival was 55 months (range: 12–140 months). We obtained death certificates of the deceased cases, and censored all causes of death that were not related to breast cancer, such as accidents, violent crimes, stroke, heart attack and liver cirrhosis, in our analysis.

Results

Tumor IHC and serum marker analysis

We examined immunohistochemically the phosphorylation status of Akt (Akt1-3) at Thr308 and Ser473, BAD at Ser136, caspase-9 at Ser196, and determined the density of CD68-positive tumor phagocytes and the expression of NOS2 and COX2 in 248 surgical specimens of breast cancer (Table I). Phosphorylation of Akt, BAD and caspase-9 are markers of Akt pathway activation, while tumor phagocyte density, and expression of NOS2 and COX2 are indicators of a proinflammatory tumor environment. We also determined the tumor HER2/neu and p53 status, because

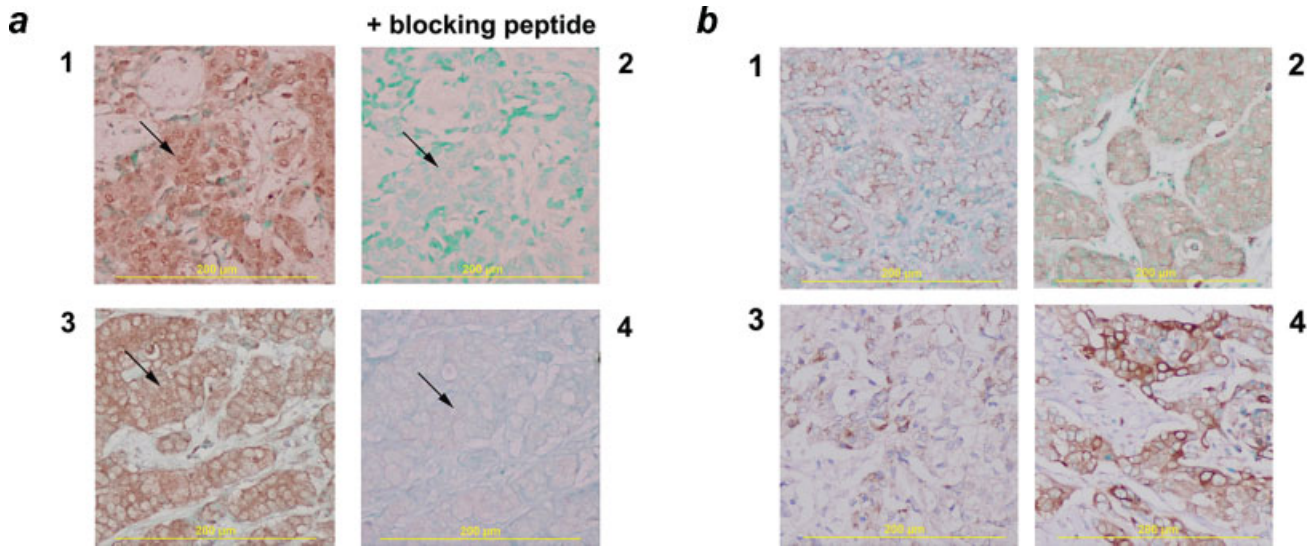

FIGURE 1 – Phosphorylation of Akt, BAD and caspase-9, and expression of NOS2 and COX2 in human breast cancer. (*a*) IHC analysis of 2 invasive ductal carcinomas for pAkt at Thr308 (1,2) and Ser473 (3,4). Arrows point to areas that are the same in panels (1,2) and (3,4). Panel 1 shows the distribution of Thr308-pAkt in tumor cells. Thr308-pAkt is both cytosolic and nuclear in distribution. The phospho-Akt (Thr308)-specific blocking peptide blocked the binding of the anti-phospho-Akt (Thr308) mouse monoclonal antibody (2). Panel 3 shows the distribution of Ser473-pAkt in tumor cells. pAkt has a cytosolic distribution with a more intensive staining at the inner cell membrane, as shown by the brown chromogen deposits. This staining is blocked after preincubation with a phospho-Akt (Ser473)-specific blocking peptide (4). (*b*) IHC analysis of invasive ductal carcinomas for Ser136-phosphorylated BAD (1), Ser196-phosphorylated caspase-9 (2), NOS2 (3) and COX2 (4). An increased phosphorylation of BAD (1) and caspase-9 (2) is seen in the cytoplasm of the tumor epithelium. The spotted distribution indicates a mitochondrial localization of the phosphorylated proteins. NOS2 (3) and COX2 (4) are expressed in the cytoplasm of tumor cells, with some cells showing a low expression while others express the proteins at very high levels. (*a*, *b*) Magnification: ×200. Counterstain: Methyl Green.

TABLE III – PHOSPHORYLATION OF AKT, BAD AND CASPASE-9 IN RELATIONSHIP TO TUMOR AND SERUM MARKERS

	P-Akt Thr308		P-Akt Ser473		P-BAD		P-Caspase-9	
	ρ[1]	*p*-value	ρ	*p*-value	ρ	*p*-value	ρ	*p*-value
Spearman rank correlation[2]								
P-Akt Thr308			0.39	<0.0001	0.4	<0.0001	0.44	<0.0001
P-Akt Ser473					0.41	<0.0001	0.5	<0.0001
P-BAD							0.51	<0.0001
NOS2	0.38	<0.0001	0.45	<0.0001	0.38	<0.0001	0.4	<0.0001
COX2	0.27	<0.0001	0.26	<0.0001	0.23	0.0003	0.36	<0.0001
CD68[3]	0.11	0.1	0.15	0.019	0.01	0.91	0.03	0.67
IGF-I[4]	0.25	0.013	0.19	0.05	0.28	0.004	0.15	0.13
IGF-I/IGFBP3	0.24	0.014	0.2	0.046	0.27	0.006	0.1	0.3
IGF-II	0.12	0.24	0.15	0.12	0.16	0.1	0.11	0.26
HER2/neu	0.17	0.008	0.22	0.0005	0.16	0.014	0.15	0.017
χ^2 test[5]								
ER (−/+)		0.72		0.41		0.35		0.7
p53 (−/+)		0.12		0.002		0.25		0.006

[1]Correlation coefficient.–[2]Calculated with IHC scores 1–4 (negative, weak, moderate, strong) and continuous data (CD68, IGF-I and II, IGF-I/IGFBP3).–[3]Tumor phagocytes.–[4]IGF-I and II, IGF-I/IGFBP3: $n = 104$.–[5]The IHC score of phosphorylated Akt, BAD and caspase-9 in breast tumors was stratified into low (negative-moderate) and high (strong) for the analysis.

both markers have previously been associated with Akt phosphorylation in breast cancer.[19,21] IGF-I, IGF-II and IGFBP3 serum concentrations were measured for the 104 cases with available serum samples (Table I). The demographic and clinicopathological data of the patients are shown in Table II.

We found a moderate to strong phosphorylation of Akt, BAD and caspase-9 in most breast tumors (Table I). The immunostaining of pAkt is shown in Figure 1*a*. The staining for the Thr308-pAkt indicated a cytosolic distribution with additional nuclear localization. Phosphorylation at Ser473 showed a cytosolic distribution with a more intensive staining at the inner cell membrane. Phosphorylated BAD and caspase-9 had a granular cytosolic distribution, which is consistent with a cytosolic and mitochondrial localization of the phosphorylated proteins (Fig. 1*b*). Phosphorylated BAD was also detected in the nucleus of tumor cells in a subset of tumors. The intensity and distribution of Akt, BAD and caspase-9 phosphorylation correlated strongly between each other (Table III). NOS2 and COX2 were expressed in both the tumor epithelium and stromal cells (Fig. 1*b*). The expression of both NOS2 and COX2 was significantly associated with tumor phagocyte density ($p = 0.016$ for NOS2 and $p = 0.01$ for COX2; Spearman rank correlation). We did not observe a correlation between serum IGF-I and markers of inflammation. Neither the expression of NOS2 and COX2, nor the density of tumor phagocytes in breast tumors, were associated with serum IGF-I (data not shown).

Akt pathway activation in relationship to markers of inflammation

We examined the relationship between the expression of NOS2 and COX2, tumor phagocyte density, and Akt pathway activation (Table III). The Spearman rank correlation analysis showed very

significant correlations between NOS2 and COX2 expression, and the phosphorylation of Akt, BAD, and caspase-9. A high expression of NOS2 and COX2 was associated with a strong phosphorylation of these proteins. We also found a correlation between HER2/neu overexpression and an increased phosphorylation of Akt, BAD and caspase-9 (Table III). The tumor phagocyte density and aberrant p53 expression were significantly associated only with the phosphorylation of Akt at Ser473, but not at Thr308. Other factors, such as ER, node, menopausal status, BMI, smoking, age, or race/ethnicity, were not associated with Akt pathway activation. We further corroborated the relationship between NOS2, COX2 and Akt pathway activation in a multivariate logistic regression analysis. NOS2 expression was an independent predictor of pAkt at Ser473 (Odds ratio (OR) = 2.9; 95% confidence interval (CI), 1.1–8.3), but not of pAkt at Thr308 (OR = 1.3; 95% CI, 0.5–4.0), in a multivariate logistic regression model that included COX2, HER2/neu, p53, IGF-I, tumor phagocytes, TNM stage and neoadjuvant therapy as covariates. COX2 expression predicted both phosphorylation at Thr308 (OR = 3.3; 95% CI, 1.2–9.4) and at Ser473 (OR = 3.0; 95% CI, 1.1–8.6) in the same multivariate analysis. The data suggest that NOS2 induces phosphorylation of Akt at Ser473, and COX2 of Akt at Thr308 and Ser473 in human breast tumors, independent of the other markers that were associated with Akt pathway activation in our study. The 2 proteins were also very significant predictors of phosphorylated caspase-9 at Ser196 (OR = 6.4; 95% CI, 1.6–25.5 and OR = 6.1; 95% CI, 1.9–20.6, respectively) in the multivariate analysis. HER2/neu overexpression, tumor phagocyte density and the tumor p53 status were not independently associated with Akt phosphorylation in our study, as judged by the logistic regression analysis (data not shown).

Akt pathway activation in relationship to IGF-I

We investigated the relationship between serum IGF-I and Akt activation in breast tumors, using both the serum IGF-I concentration and the ratio between IGF-I and IGFBP3 as indicators of IGF-I bioavailability. Both IGF-I and the IGF-I/IGFBP3 ratio showed very similar and statistically significant associations with the phosphorylation status of Akt and BAD in tumor tissues (Table III). The observed association with Akt phosphorylation at Thr308 was independent of other markers that were associated with protein phosphorylation in our study. The multivariate logistic regression analysis showed that serum IGF-I and the IGF-I/IGFBP3 ratio were predictors of Akt phosphorylation at Thr308 (OR = 5.2; 95% CI, 1.7–16.5 and OR = 2.9; 95% CI, 1.1–7.8, respectively), after adjustment for IGF-II, NOS2, COX2, HER2/neu, p53, tumor phagocytes, TNM stage and neoadjuvant therapy. The association with Akt phosphorylation at Ser473 was weaker and not statistically significant in the multivariate analysis. We also examined the correlation between serum IGF-II and Akt phosphorylation to discriminate between the effect of serum IGF-I and IGF-II with respect to Akt activation in breast tumors. Serum IGF-II was not significantly associated with Akt pathway activation in our study (Table III).

Phosphorylation of Akt in human breast cancer cells treated with nitric oxide and prostaglandin E_2

We further investigated the relationship between NOS2 and COX2 activity and pAkt, and assessed whether the major metabolites of NOS2 and COX2 induce the phosphorylation of Akt at Thr308 and Ser473. We examined the effect of nitric oxide and prostaglandin E_2 on Akt phosphorylation in human breast cancer cells. MCF-7 and MDA-MB-231 cells were treated with 25 μM SPER/NO, a nitric oxide donor, for 1–4 hr, (Fig. 2*a*). At this concentration, SPER/NO generates 100–400 nM nitric oxide concentrations in the cell culture medium. Both cell lines contained detectable amounts of pAkt at Ser473 at baseline. Nitric oxide increased Akt phosphorylation at Ser473 but did not lead to a detectable enhancement of the phosphorylation at Thr308 in the 2 cell lines. We also observed an induction of Akt phosphorylation at Ser473 by nitric oxide in a third breast cancer cell line, MDA-MB-157. Prostaglandin E_2, the most active proinflammatory metabolite of COX2, stimulated Akt pathway activation as well (Fig. 2*b*). At a 5 μM concentration, prostaglandin E_2 induced Akt phosphorylation at Ser473 and GSK-3β at Ser9, a known downstream target of pAkt, in both cell lines. The prostaglandin E_2 response appeared to be stronger in MDA-MB-231 cells than in MCF-7 cells.

Treatment of human breast cancer cells with okadaic acid

To test whether Akt phosphorylation may lead to an induction of NOS2 and COX2 expression, we treated MCF-7 cells and MDA-MB-231 cells with 10 and 100 nM okadaic acid, respectively. In the initial titration experiment with 0, 10, 100, 300 nM okadaic acid, these 2 concentrations induced a similar phosphorylation of Akt at Ser473 in the 2 cell lines (data not shown). Okadaic acid is an inhibitor of the protein phosphatase 2A and leads to an accumulation of pAkt and activation of the Akt pathway.[31,32] We exposed cells for 48 hr time to okadaic acid, and examined the induction of NOS2 and COX2 by Western blot analysis (Fig. 2*c*). As expected, okadaic acid induced the activation of the Akt pathway, as shown by the phosphorylation of Akt at Ser473 and GSK3β at Ser9. We could not detect an induction of NOS2 in the 2 cell lines, but observed an induction of COX2 at 48 hr in MDA-MB-231 cells (Fig. 2*c*). The data suggest that Akt pathway activation in human breast cancer cells does not lead to an induction of NOS2. Akt activation, however, appears to induce the expression of COX2 in at least some breast cancer cells.

Coculture of human breast cancer cells with ANA-1 macrophages

We used a coculture experiment with human breast cancer cells and ANA-1 mouse macrophages to corroborate the association between tumor phagocytes and pAkt in breast tumors. We found that ANA-1 mouse macrophages induce phosphorylation of Akt in MCF-7 cells during a time course of 1–4 hr (Fig. 3*a*). The detected phosphorylation at Ser473 appeared to be much stronger than the phosphorylation at Thr308. The induction was not dependent on the activation status of the macrophages; untreated and INF-γ/LPS-stimulated macrophages induced pAkt to a similar extent. We repeated the coculture experiment with a second breast cancer cell line, MDA-MB-231. Again, we found that unstimulated ANA-1 cells induced a phosphorylation of Akt that appeared to be stronger at Ser473 than at Thr308 (Fig. 3*b*).

Akt pathway activation and breast cancer survival

We investigated the association between Akt pathway activation and overall survival, and focused on the inhibition of apoptosis as a predictor of outcome. We censored all causes of death that were not related to breast cancer. Hence, overall survival in our study meets the definition of breast cancer survival.

We first studied the association between the phosphorylation status of Akt, BAD and caspase-9, and the breast cancer outcome using Kaplan–Meier survival analysis (Fig. 4). The Kaplan–Meier method and the log-rank test did not show an association between the phosphorylation status of Akt, BAD and caspase-9 in breast tumors, and breast cancer survival. This did not change when we dichotomized the data at a different cutoff point, using the immunostaining score of moderate to strong, instead of strong, to define high protein phosphorylation. We further corroborated our observations with a multivariate analysis, using the Cox Proportional-Hazards Regression and adjustments for age at diagnosis, race, BMI, ER status, TNM stage and chemotherapy. In this analysis, neither phosphorylation of Akt, BAD or caspase-9 was significantly associated with breast cancer outcome.

Because we hypothesized that tissue inflammation may biologically interact with the Akt pathway in breast tumors and modify the effect of the Akt phosphorylation status on breast cancer survival, we stratified our survival analysis by tumor phagocyte density. We observed that the tumor phagocyte density modified the effect of Akt phosphorylation on breast cancer survival in our

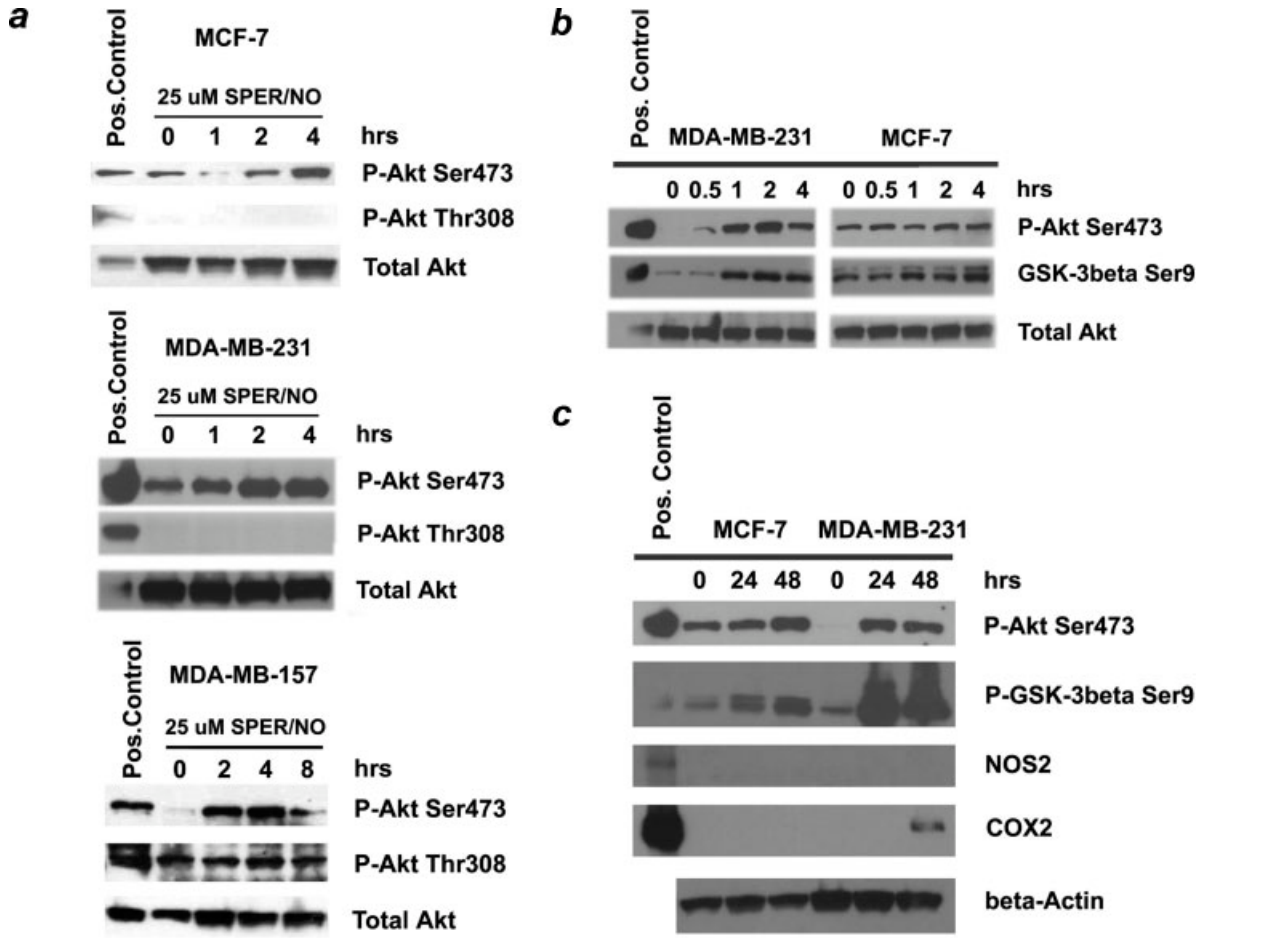

FIGURE 2 – Treatment of human breast cancer cells with nitric oxide, prostaglandin E_2 and okadaic acid. The nitric oxide-donor, SPER/NO, induces Akt phosphorylation in human breast cancer cells (*a*). MCF-7, MDA-MB-231 and MDA-MB-157 cells were treated with 25 μM SPER/NO for 4 and 8 hr. The phosphorylation of Akt at Ser473, but not Thr308, increased during the time course. Prostaglandin E_2 induces Akt and GSK-3β phosphorylation in human breast cancer cells (*b*). MCF-7 cells and MDA-MB-231 cells were treated with 5 μM prostaglandin E_2 for 0.5, 1, 2, 4 hr. The treatment caused phosphorylation of Akt and GSK-3β in both cell lines, but the induction was stronger in MDA-MB-231 cells than in MCF-7 cells. Ser9 in GSK-3β is a downstream target of Akt. Okadaic acid induces COX2, but not NOS2 expression in human breast cancer cells (*c*). MCF-7 cells and MDA-MB-231 cells were treated with 10 and 100 nM okadaic acid, respectively, for 24 and 48 hr. Treatment with okadaic acid, a phosphatase 2A inhibitor, induced the phosphorylation of Akt at Ser473 and GSK-3β at Ser9. Okadaic acid also stimulated the expression of COX2 in MDA-MB-231 cells. Okadaic acid treatment did not lead to an upregulation of NOS2. Cell extracts were prepared and 50 μg of total protein were loaded per lane on an 8% gel for Western blot analysis.

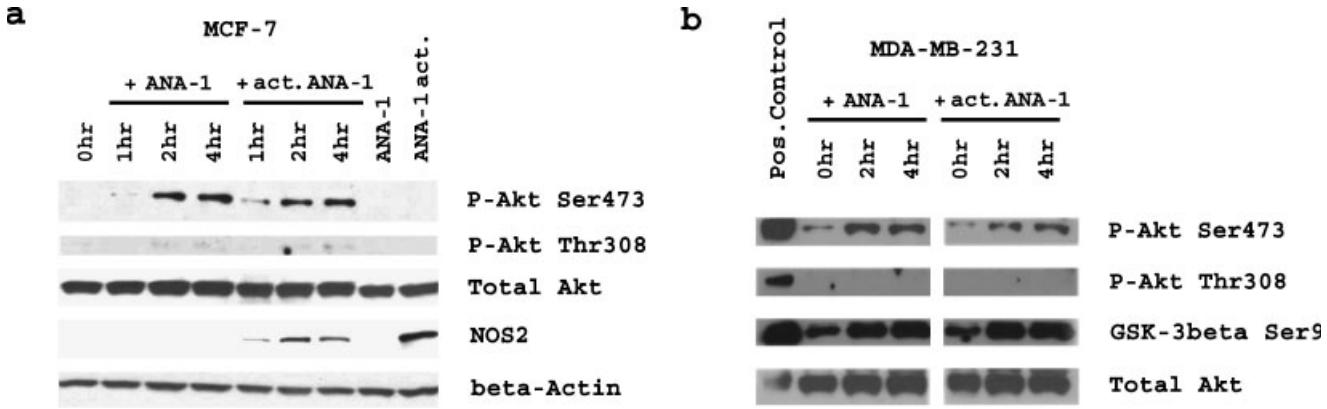

FIGURE 3 – ANA-1 macrophages induce Akt phosphorylation in human breast cancer cells. ANA-1 cells induced a strong phosphorylation of Akt at Ser473 and a weaker phosphorylation at Thr308 in MCF-7 cells (*a*) and MDA-MB-231 cells (*b*), after coculture for 1, 2 and 4 hr. Protein phosphorylation was induced by both untreated ANA-1 cells and by interferon-γ/LPS-stimulated ANA-1 cells. The coculture conditions are described under Material and Methods. In the experiments with MDA-MB-231 cells, ANA-1 cells were separated from the breast cancer cells using a spin column (see Methods). Fifty micrograms of total protein was loaded per lane on an 8% gel for Western blot analysis.

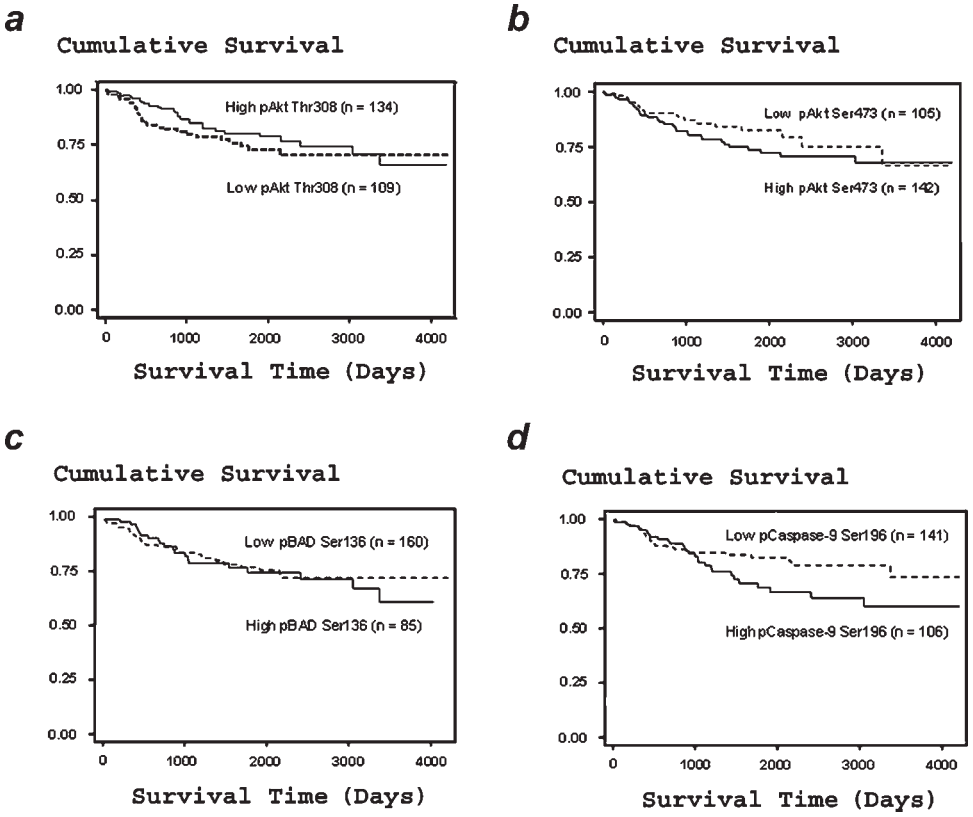

FIGURE 4 – Kaplan–Meier survival analysis according to the phosphorylation status of Akt at Thr308 and Ser473, BAD at Ser136, and caspase-9 at Ser196 in breast tumors. Shown are the Kaplan–Meier curves (*a–d*). Dashed line: low protein phosphorylation. Solid line: high protein phosphorylation. Patients who have a high phosphorylation of Akt, BAD and caspase-9 in their breast tumors have an overall survival that is not significantly different from the overall survival of patients who show a low protein phosphorylation. Log-rank test for equality of survival curves, $p = 0.39$ (*a*), 0.27 (*b*), 0.75 (*c*) and 0.11 (*d*). Low phosphorylation: negative-moderate IHC staining; high phosphorylation: strong IHC staining.

TABLE IV – ASSOCIATION BETWEEN TUMOR AKT PHOSPHORYLATION AND OVERALL SURVIVAL AFTER STRATIFICATION BY TUMOR PHAGOCYTE COUNT

	n	HR[1]	*p*-value	HR[2]	*p*-value
Akt Thr308					
All cases	188	0.7 (0.4–1.2)	0.2	0.8 (0.6–1.1)	0.12
Tumor phagocytes					
< Median count	94	1.8 (0.7–4.6)	0.26	1.1 (0.6–1.9)	0.84
Tumor phagocytes					
≥ Median count	94	0.2 (0.1–0.6)	0.002	0.5 (0.3–0.8)	0.006
Neoadjuvant therapy					
No	65	0.3 (0.1–1.4)	0.14	0.4 (0.1–0.9)	0.03
Yes	29	0.1 (0.01–0.3)	0.001	0.5 (0.3–0.9)	0.02
Akt Ser473					
All cases	193	0.9 (0.5–1.7)	0.8	0.9 (0.6–1.3)	0.55
Tumor phagocytes					
< Median count	96	2.0 (0.7–5.9)	0.19	1.4 (0.7–2.7)	0.3
Tumor phagocytes					
≥ Median count	97	0.5 (0.2–1.1)	0.09	0.6 (0.3–0.9)	0.03
Neoadjuvant therapy					
No	68	1.4 (0.3–5.4)	0.65	0.9 (0.4–2.3)	0.82
Yes	29	0.2 (0.1–0.7)	0.01	0.4 (0.2–0.8)	0.01

Cox Proportional-Hazards regression adjusted for age at diagnosis, race, BMI, estrogen receptor, TNM stage and chemotherapy.

[1]Hazard ratio (HR) and 95% confidence interval (CI) comparing strong IHC *versus* negative-moderate IHC as the reference group.–[2]HR with IHC entered as categorized data (1, 2, 3, 4 = negative, weak, moderate, strong). Values in parentheses indicate 95% confidence intervals.

study population (Table IV). In tumors with an above median phagocyte count, a high pAkt was found to be associated with improved survival. This finding was statistically significant for the Thr308 phosphorylation and suggestive for the Ser473 phosphorylation. Because of this unexpected result, we further stratified by cancer treatment. The stratification indicated that the association could be related to neoadjuvant therapy (Table IV). We corroborated our finding with a statistical test for interaction. Consistent with the survival analysis, we found statistical interactions between Akt phosphorylation at Thr308 and Ser473, and tumor phagocyte density on breast cancer survival ($p_{interaction} < 0.05$, respectively). The interaction was particularly strong in the subgroup of patients who received neoadjuvant therapy ($p_{interaction} = 0.001$ and $p_{interaction} = 0.01$, respectively).

Discussion

We studied the phosphorylation of Akt, BAD and caspase-9 in 248 surgical breast tumors by IHC analysis and found that most breast tumors have moderate to high levels of pAkt, BAD and cas-

pase-9. To our best knowledge, this is the first study that assessed the phosphorylation status of BAD and caspase-9 in human breast tumors. A deregulation of the PI3K pathway is the most common genetic alteration in breast cancer with 10–35% of breast tumors having a diminished PTEN expression, while another 25–30% may harbor a *PIK3CA* mutation.[33–35] These genetic changes are thought to result in a constitutive activation of the Akt pathway. Our data are consistent with these findings by showing that a moderate to strong phosphorylation of Akt, BAD and caspase-9 is frequent in human breast tumors.

The intensity and distribution of Akt, BAD and caspase-9 phosphorylation correlated strongly between each other. The finding is an additional validation of the IHC results, because the phosphorylation of Akt at Ser473 and Thr308 are sequential steps that lead to kinase activation and phosphorylation of downstream targets, such as BAD and caspase-9.[1] We found that Ser473-pAkt was partly membrane-bound and Thr308-pAkt had a predominantly cytosolic and nuclear localization. The observations are in agreement with the model that Ser473 phosphorylation precedes Thr308 phosphorylation, which leads to membrane detachment and nuclear translocation.[9,10] We observed a cytosolic and mitochondrial localization of phosphorylated BAD and caspase-9, and also a nuclear localization of phosphorylated BAD in a subset of the breast tumors. BAD and caspase-9 are both mitochondrial proteins that redistribute from the mitochondria to the cytosol upon stress or protein phosphorylation.[13–15,36] Thus, our IHC results are consistent with the reported localization of these phosphorylated proteins in cell culture.

Phosphorylation of Akt, BAD and caspase-9 is a sequence that activates a survival pathway and raises the threshold for apoptosis. The phosphorylation of BAD and caspase-9 inhibits their proapoptotic function.[13–15] We observed that 3 markers of a proinflammatory environment, the expression of NOS2 and COX2, and the tumor phagocyte density, were associated with the phosphorylation of Akt, BAD and caspase-9 in breast tumors. The tumor phagocyte density was significantly associated with the phosphorylation of Akt at Ser473; however, the association was not independent of other tumor markers in the multivariate analysis. Phagocytes express NOS2 and can produce high amounts of nitric oxide.[37] Our multivariate analysis indicated that NOS2 is a confounder of the relationship between tumor phagocytes and Akt phosphorylation, suggesting that the release of nitric oxide by tumor phagocytes may induce the phosphorylation of Akt at Ser473 in the tumor epithelium.

NOS2 and COX2 were both independently associated with Akt pathway activation in the multivariate analysis, after adjustment for potential confounders; however, NOS2 expression only predicted the Ser473 phosphorylation, while COX2 expression predicted both Thr308 and Ser473 phosphorylation of Akt. The data indicate that both enzymes activate the Akt pathway in a dominant manner in human breast tumors but NOS2 may primarily induce the phosphorylation of Ser473. Alternatively, pAkt may have led to the upregulation of NOS2 and COX2 in breast tumors. We found that the activation of the Akt pathway by the phosphatase 2A-inhibitor, okadaic acid,[31,32] induces COX2 expression in MDA-MB-231 human breast cancer cells. Okadaic acid did not stimulate the expression of NOS2 in this cell line or another human breast cancer cell line, MCF-7. Furthermore, it has previously been shown for COX2, but not NOS2, that Akt activation is involved in the transcriptional upregulation of the enzyme in human cells.[38] Thus, pAkt may induce COX2 expression in human breast tumors. However, the expression of a COX2 transgene induces Akt phosphorylation in human cells,[39] and several recent studies have shown that COX2-specific inhibitors block Akt phosphorylation and disrupt Akt signaling in various cancer cell lines,[22,40,41] supporting the hypothesis that COX2 upregulation, as part of an inflammatory response, leads to Akt phosphorylation in human tumors. Additionally, the proinflammatory COX2 metabolite, prostaglandin E_2, has been shown to induce Akt phosphorylation in colon cancer cells.[42] We exposed breast cancer cells to prostaglandin E_2 and detected the phosphorylation of Akt and GSK-3β, a downstream target of pAkt.[1] These data indicate that COX2 and its major proinflammatory metabolite, prostaglandin E_2, stimulate Akt pathway activation in human cancer cells.

We also extended our finding that NOS2 expression and phagocytes may induce pAkt in breast cancer cells, with a preference for Ser473. The nitric oxide donor, SPER/NO, induced a detectable phosphorylation only at Ser473 in MCF-7, MDA-MB-231 and MDA-MB-157 human breast carcinoma cells. ANA-1 mouse macrophages stimulated a strong phosphorylation at Ser473 in both MCF-7 and MDA-MB-231 cells, but an increase in the phosphorylation of Thr308 was either undetectable or weak in our coculture experiments. It was not shown previously that phagocytes and nitric oxide induce Akt phosphorylation in human cancer cells but DETA/NO, a nitric oxide donor closely related to SPER/NO, was found to induce Akt Ser473 phosphorylation in RINm5F cells.[43]

Serum IGF-I was found to be associated with an increased breast cancer risk in population-based studies.[6,23] Although epidemiological and experimental studies indicate that IGF-I activates cancer-related pathways, an association between IGF-I and breast cancer outcome has not been reported, and very few studies attempted to link serum IGF-I to pathway activation in human tissue specimens. We hypothesized that IGF-I may induce low-level tissue inflammation[24,25,44] and activate the Akt pathway. We did not observe an association between serum IGF-I concentrations and markers of inflammation in breast tumors, but found that serum IGF-I and the IGF-I/IGFBP3 ratio, a measure for bioavailable IGF-I, were associated with Akt pathway activation and predicted Akt phosphorylation at Thr308 in human breast tumors. Our data indicate that breast cancer patients with a high serum concentration of bioavailable IGF-I, either because of a genetic predisposition or because of their lifestyle,[6] are more likely to have a strong phosphorylation of Akt in their tumors than those with a low concentration of bioavailable IGF-I. We did not find that IGF-I independently predicted the phosphorylation of Akt at Ser473, although it was shown to induce Akt phosphorylation at both Thr308 and Ser473 in cell culture.[10,45] It is possible that other pathways have a more dominant effect on the phosphorylation of Ser473 in breast tumors. IGF-I induces a transcriptional profile in breast epithelial cells that is consistent with the induction of angiogenesis and cancer progression.[46] There is strong evidence, from inhibitor and knockout studies, that the IGF-I receptor promotes adhesion, invasion, metastasis, survival and drug-resistance of breast cancer cells.[47–49] Our finding from human breast tumors are in agreement with cell culture-based observations that IGF-I activates the Akt survival pathway in cancer cells.

Previous studies investigated the association between the PI3K pathway and breast cancer outcome. Several studies found an association between Akt Ser473 phosphorylation and disease-free survival and/or the response to therapy in breast cancer.[19–21] Another study reported that the loss of PTEN predicts trastuzumab resistance in breast cancer patients.[50] However, 2 large studies did not observe an association between breast cancer survival and either *PI3CA* mutations, *PTEN* loss, or Akt Ser473 phosphorylation.[34,51] We could not study disease-free survival. Instead, we examined overall survival that was censored for deaths not related to breast cancer to meet the definition of breast cancer-specific survival. We did not find a significant association between Akt, BAD and caspase-9 phosphorylation, and breast cancer outcome in the univariate and multivariate analyses. The data suggests that Akt pathway activation may not be associated with overall survival in breast cancer in an unstratified analysis.

Because we hypothesized *a priori* that inflammation may interact with the Akt pathway in breast cancer survival, we performed further analyses and studied whether tumor phagocyte density modifies the association between the Akt phosphorylation status and breast cancer survival. We found a statistical interaction between pAkt and tumor phagocyte count on breast cancer survival, and observed that Akt phosphorylation was associated with increased breast cancer survival if the tumor phagocyte count was

high. This relationship was particularly strong in patients who had received neoadjuvant therapy. This is a preliminary finding. Because of the exploratory nature of our analysis, we cannot exclude the possibility that the observed interaction is a chance finding. Therefore, further confirmation in other studies is needed to determine whether a proinflammatory tumor environment modifies the association between the Akt phosphorylation status and breast cancer survival.

We used CD68 as a marker for phagocyte infiltration. CD68 is expressed in cells of the mononuclear phagocyte lineage and is thought to be the best panmacrophage marker.[52] Tumor-associated macrophages can be both tumoricidal and protumor.[53,54] A high density of phagocytes in tumors may cause cytotoxicity, angiostasis and tumor regression.[55] Thus, the high phagocyte infiltration after neoadjuvant therapy may not only lead to an increased phosphorylation of Akt in breast tumors, but also to a strong antitumor response. Our data suggest that, in this environment of excessive inflammation, Akt signaling can be detrimental to tumor progression. It has recently been shown that the PI3K pathway can augment p53 tumor suppressor activity in chemotherapy-treated cells.[56] There is also new evidence that activation of Akt1 can suppress tumor invasion.[57–59] The data indicate that Akt pathway activation may not always promote tumor progression. If Akt activation would promote survival but also inhibit tumor invasion, this could explain why Akt phosphorylation is associated with poor disease-free survival, but not overall survival, in human breast cancer.

In summary, we found that a proinflammatory environment and serum IGF-I are markers of Akt pathway activation in breast cancer. The expression of NOS2 and COX2, and a high tumor phagocyte density, were associated with increased Akt phosphorylation in human breast tumors. Additional experiments with human breast cancer cells corroborated these findings.

Acknowledgements

The authors thank Mr. Neil Caporaso for his help with the study design and Mrs. Melissa Miller for help with the statistical analysis. We also thank Mr. Raymond Jones, Ms. Audrey Salabes, Mr. Leoni Leondaridis, Mr. Glennwood Trivers, Mrs. Elise Bowman, and personnel at the University of Maryland and the Baltimore Veterans Administration, and the Surgery and Pathology Departments at the University of Maryland Medical Center, Baltimore Veterans Affairs Medical Center, Union Memorial Hospital, Mercy Medical Center and Sinai Hospital for their contributions.

References

1. Brazil DP, Hemmings BA. Ten years of protein kinase B signalling: a hard Akt to follow. Trends Biochem Sci 2001;26:657–64.
2. Mayo LD, Donner DB. The PTEN, Mdm2, p53 tumor suppressor-oncoprotein network. Trends Biochem Sci 2002;27:462–7.
3. Liu H, Radisky DC, Wang F, Bissell MJ. Polarity and proliferation are controlled by distinct signaling pathways downstream of PI3-kinase in breast epithelial tumor cells. J Cell Biol 2004;164:603–12.
4. Zhao JJ, Gjoerup OV, Subramanian RR, Cheng Y, Chen W, Roberts TM, Hahn WC. Human mammary epithelial cell transformation through the activation of phosphatidylinositol 3-kinase. Cancer Cell 2003;3:483–95.
5. Debnath J, Walker SJ, Brugge JS. Akt activation disrupts mammary acinar architecture and enhances proliferation in an mTOR-dependent manner. J Cell Biol 2003;163:315–26.
6. Pollak MN, Schernhammer ES, Hankinson SE. Insulin-like growth factors and neoplasia. Nat Rev Cancer 2004;4:505–18.
7. Sarbassov DD, Guertin DA, Ali SM, Sabatini DM. Phosphorylation and regulation of Akt/PKB by the rictor-mTOR complex. Science 2005;307:1098–101.
8. Stephens L, Anderson K, Stokoe D, Erdjument-Bromage H, Painter GF, Holmes AB, Gaffney PR, Reese CB, McCormick F, Tempst P, Coadwell J, Hawkins PT. Protein kinase B kinases that mediate phosphatidylinositol 3,4,5-trisphosphate-dependent activation of protein kinase B. Science 1998;279:710–14.
9. Scheid MP, Marignani PA, Woodgett JR. Multiple phosphoinositide 3-kinase-dependent steps in activation of protein kinase B. Mol Cell Biol 2002;22:6247–60.
10. Andjelkovic M, Alessi DR, Meier R, Fernandez A, Lamb NJ, Frech M, Cron P, Cohen P, Lucocq JM, Hemmings BA. Role of translocation in the activation and function of protein kinase B. J Biol Chem 1997;272:31515–24.
11. Zhou BP, Hung MC. Novel targets of Akt, p21(Cipl/WAF1), and MDM2. Semin Oncol 2002;29:62–70.
12. Shin I, Yakes FM, Rojo F, Shin NY, Bakin AV, Baselga J, Arteaga CL. PKB/Akt mediates cell-cycle progression by phosphorylation of p27(Kip1) at threonine 157 and modulation of its cellular localization. Nat Med 2002;8:1145–52.
13. Cardone MH, Roy N, Stennicke HR, Salvesen GS, Franke TF, Stanbridge E, Frisch S, Reed JC. Regulation of cell death protease caspase-9 by phosphorylation. Science 1998;282:1318–21.
14. Datta SR, Dudek H, Tao X, Masters S, Fu H, Gotoh Y, Greenberg ME. Akt phosphorylation of BAD couples survival signals to the cell-intrinsic death machinery. Cell 1997;91:231–41.
15. Datta SR, Ranger AM, Lin MZ, Sturgill JF, Ma YC, Cowan CW, Dikkes P, Korsmeyer SJ, Greenberg ME. Survival factor-mediated BAD phosphorylation raises the mitochondrial threshold for apoptosis. Dev Cell 2002;3:631–43.
16. Simoncini T, Hafezi-Moghadam A, Brazil DP, Ley K, Chin WW, Liao JK. Interaction of oestrogen receptor with the regulatory subunit of phosphatidylinositol-3-OH kinase. Nature 2000;407:538–41.
17. Bacus SS, Altomare DA, Lyass L, Chin DM, Farrell MP, Gurova K, Gudkov A, Testa JR. AKT2 is frequently upregulated in HER-2/neu-positive breast cancers and may contribute to tumor aggressiveness by enhancing cell survival. Oncogene 2002;21:3532–40.
18. Zhou BP, Liao Y, Xia W, Zou Y, Spohn B, Hung MC. HER-2/neu induces p53 ubiquitination via Akt-mediated MDM2 phosphorylation. Nat Cell Biol 2001;3:973–82.
19. Zhou X, Tan M, Stone HV, Klos KS, Lan KH, Yang Y, Yang W, Smith TL, Shi D, Yu D. Activation of the Akt/mammalian target of rapamycin/4E-BP1 pathway by ErbB2 overexpression predicts tumor progression in breast cancers. Clin Cancer Res 2004;10:6779–88.
20. Perez-Tenorio G, Stal O. Activation of AKT/PKB in breast cancer predicts a worse outcome among endocrine treated patients. Br J Cancer 2002;86:540–5.
21. Vestey SB, Sen C, Calder CJ, Perks CM, Pignatelli M, Winters ZE. Activated Akt expression in breast cancer: correlation with p53, Hdm2 and patient outcome. Eur J Cancer 2005;41:1017–25.
22. Kucab JE, Lee C, Chen CS, Zhu J, Gilks CB, Cheang M, Huntsman D, Yorida E, Emerman J, Pollak M, Dunn SE. Celecoxib analogues disrupt Akt signaling, which is commonly activated in primary breast tumours. Breast Cancer Res 2005;7:R796–R807.
23. Renehan AG, Zwahlen M, Minder C, O'Dwyer ST, Shalet SM, Egger M. Insulin-like growth factor (IGF)-I, IGF binding protein-3, and cancer risk: systematic review and meta-regression analysis. Lancet 2004;363:1346–53.
24. Heemskerk VH, Daemen MA, Buurman WA. Insulin-like growth factor-1 (IGF-1) and growth hormone (GH) in immunity and inflammation. Cytokine Growth Factor Rev 1999;10:5–14.
25. Di Popolo A, Memoli A, Apicella A, Tuccillo C, di Palma A, Ricchi P, Acquaviva AM, Zarrilli R. IGF-II/IGF-I receptor pathway up-regulates COX-2 mRNA expression and PGE2 synthesis in Caco-2 human colon carcinoma cells. Oncogene 2000;19:5517–24.
26. Che W, Lerner-Marmarosh N, Huang Q, Osawa M, Ohta S, Yoshizumi M, Glassman M, Lee JD, Yan C, Berk BC, Abe J. Insulin-like growth factor-1 enhances inflammatory responses in endothelial cells: role of Gab1 and MEKK3 in TNF-α-induced c-Jun and NF-kappaB activation and adhesion molecule expression. Circ Res 2002;90:1222–30.
27. Boersma BJ, Howe TM, Goodman JE, Yfantis HG, Lee DH, Chanock SJ, Ambs S. Association of breast cancer outcome with status of p53 and MDM2 SNP309. J Natl Cancer Inst 2006;98:911–19.
28. Burke L, Flieder DB, Guinee DG, Brambilla E, Freedman AN, Bennett WP, Jones JT, Borkowski A, Caporaso NA, Fleming M, Trastek V, Pairolero P et al. Prognostic implications of molecular and immunohistochemical profiles of the Rb and p53 cell cycle regulatory pathways in primary non-small cell lung carcinoma. Clin Cancer Res 2005;11:232–41.
29. Vakkala M, Kahlos K, Lakari E, Paakko P, Kinnula V, Soini Y. Inducible nitric oxide synthase expression, apoptosis, and angiogenesis in in situ and invasive breast carcinomas. Clin Cancer Res 2000;6:2408–16.
30. Hofseth LJ, Saito S, Hussain SP, Espey MG, Miranda KM, Araki Y, Jhappan C, Higashimoto Y, He P, Linke SP, Quezado MM, Zurer I et al. Nitric oxide-induced cellular stress and p53 activation in chronic inflammation. Proc Natl Acad Sci USA 2003;100:143–8.

31. Resjo S, Goransson O, Harndahl L, Zolnierowicz S, Manganiello V, Degerman E. Protein phosphatase 2A is the main phosphatase involved in the regulation of protein kinase B in rat adipocytes. Cell Signal 2002;14:231–8.
32. Andjelkovic M, Jakubowicz T, Cron P, Ming XF, Han JW, Hemmings BA. Activation and phosphorylation of a pleckstrin homology domain containing protein kinase (RAC-PK/PKB) promoted by serum and protein phosphatase inhibitors. Proc Natl Acad Sci USA 1996;93: 5699–704.
33. Perren A, Weng LP, Boag AH, Ziebold U, Thakore K, Dahia PL, Komminoth P, Lees JA, Mulligan LM, Mutter GL, Eng C. Immunohistochemical evidence of loss of PTEN expression in primary ductal adenocarcinomas of the breast. Am J Pathol 1999;155:1253–60.
34. Saal LH, Holm K, Maurer M, Memeo L, Su T, Wang X, Yu JS, Malmstrom PO, Mansukhani M, Enoksson J, Hibshoosh H, Borg A et al. PIK3CA mutations correlate with hormone receptors, node metastasis, and ERBB2, and are mutually exclusive with PTEN loss in human breast carcinoma. Cancer Res 2005;65:2554–9.
35. Campbell IG, Russell SE, Choong DY, Montgomery KG, Ciavarella ML, Hooi CS, Cristiano BE, Pearson RB, Phillips WA. Mutation of the PIK3CA gene in ovarian and breast cancer. Cancer Res 2004; 64:7678–81.
36. Susin SA, Lorenzo HK, Zamzami N, Marzo I, Brenner C, Larochette N, Prevost MC, Alzari PM, Kroemer G. Mitochondrial release of caspase-2 and -9 during the apoptotic process. J Exp Med 1999;189:381–94.
37. MacMicking J, Xie QW, Nathan C. Nitric oxide and macrophage function. Annu Rev Immunol 1997;15:323–50.
38. St Germain ME, Gagnon V, Mathieu I, Parent S, Asselin E. Akt regulates COX-2 mRNA and protein expression in mutated-PTEN human endometrial cancer cells. Int J Oncol 2004;24:1311–24.
39. Leng J, Han C, Demetris AJ, Michalopoulos GK, Wu T. Cyclooxygenase-2 promotes hepatocellular carcinoma cell growth through Akt activation: evidence for Akt inhibition in celecoxib-induced apoptosis. Hepatology 2003;38:756–68.
40. Wu T, Leng J, Han C, Demetris AJ. The cyclooxygenase-2 inhibitor celecoxib blocks phosphorylation of Akt and induces apoptosis in human cholangiocarcinoma cells. Mol Cancer Ther 2004;3:299–307.
41. Hsu AL, Ching TT, Wang DS, Song X, Rangnekar VM, Chen CS. The cyclooxygenase-2 inhibitor celecoxib induces apoptosis by blocking Akt activation in human prostate cancer cells independently of Bcl-2. J Biol Chem 2000;275:11397–403.
42. Castellone MD, Teramoto H, Williams BO, Druey KM, Gutkind JS. Prostaglandin E2 promotes colon cancer cell growth through a Gs-axin-β-catenin signaling axis. Science 2005;310:1504–10.
43. Tejedo JR, Cahuana GM, Ramirez R, Esbert M, Jimenez J, Sobrino F, Bedoya FJ. Nitric oxide triggers the phosphatidylinositol 3-kinase/Akt survival pathway in insulin-producing RINm5F cells by arousing Src to activate insulin receptor substrate-1. Endocrinology 2004;145: 2319–27.
44. Weisberg SP, McCann D, Desai M, Rosenbaum M, Leibel RL, Ferrante AW, Jr. Obesity is associated with macrophage accumulation in adipose tissue. J Clin Invest 2003;112:1796–808.
45. Alessi DR, Andjelkovic M, Caudwell B, Cron P, Morrice N, Cohen P, Hemmings BA. Mechanism of activation of protein kinase B by insulin and IGF-1. EMBO J 1996;15:6541–51.
46. Oh JS, Kucab JE, Bushel PR, Martin K, Bennett L, Collins J, DiAugustine RP, Barrett JC, Afshari CA, Dunn SE. Insulin-like growth factor-1 inscribes a gene expression profile for angiogenic factors and cancer progression in breast epithelial cells. Neoplasia 2002;4:204–17.
47. Dunn SE, Ehrlich M, Sharp NJ, Reiss K, Solomon G, Hawkins R, Baserga R, Barrett JC. A dominant negative mutant of the insulin-like growth factor-I receptor inhibits the adhesion, invasion, and metastasis of breast cancer. Cancer Res 1998;58:3353–61.
48. Sachdev D, Hartell JS, Lee AV, Zhang X, Yee D. A dominant negative type I insulin-like growth factor receptor inhibits metastasis of human cancer cells. J Biol Chem 2004;279:5017–24.
49. Burtrum D, Zhu Z, Lu D, Anderson DM, Prewett M, Pereira DS, Bassi R, Abdullah R, Hooper AT, Koo H, Jimenez X, Johnson D et al. A fully human monoclonal antibody to the insulin-like growth factor I receptor blocks ligand-dependent signaling and inhibits human tumor growth in vivo. Cancer Res 2003;63:8912–21.
50. Nagata Y, Lan KH, Zhou X, Tan M, Esteva FJ, Sahin AA, Klos KS, Li P, Monia BP, Nguyen NT, Hortobagyi GN, Hung MC et al. PTEN activation contributes to tumor inhibition by trastuzumab, and loss of PTEN predicts trastuzumab resistance in patients. Cancer Cell 2004; 6:117–27.
51. Panigrahi AR, Pinder SE, Chan SY, Paish EC, Robertson JF, Ellis IO. The role of PTEN and its signalling pathways, including AKT, in breast cancer; an assessment of relationships with other prognostic factors and with outcome. J Pathol 2004;204:93–100.
52. Greaves DR, Gordon S. Macrophage-specific gene expression: current paradigms and future challenges. Int J Hematol 2002;76:6–15.
53. Bingle L, Brown NJ, Lewis CE. The role of tumour-associated macrophages in tumour progression: implications for new anticancer therapies. J Pathol 2002;196:254–65.
54. Lewis CE, Pollard JW. Distinct role of macrophages in different tumor microenvironments. Cancer Res 2006;66:605–12.
55. Coussens LM, Werb Z. Inflammation and cancer. Nature 2002;420: 860–7.
56. Bar J, Lukaschuk N, Zalcenstein A, Wilder S, Seger R, Oren M. The PI3K inhibitor LY294002 prevents p53 induction by DNA damage and attenuates chemotherapy-induced apoptosis. Cell Death Differ 2005; 12:1578–87.
57. Hutchinson JN, Jin J, Cardiff RD, Woodgett JR, Muller WJ. Activation of Akt-1 (PKB-α) can accelerate ErbB-2-mediated mammary tumorigenesis but suppresses tumor invasion. Cancer Res 2004;64: 3171–8.
58. Yoeli-Lerner M, Yiu GK, Rabinovitz I, Erhardt P, Jauliac S, Toker A. Akt blocks breast cancer cell motility and invasion through the transcription factor NFAT. Mol Cell 2005;20:539–50.
59. Irie HY, Pearline RV, Grueneberg D, Hsia M, Ravichandran P, Kothari N, Natesan S, Brugge JS. Distinct roles of Akt1 and Akt2 in regulating cell migration and epithelial-mesenchymal transition. J Cell Biol 2005;171:1023–34.